INDIAN JOURNAL OF SCIENCE AND TECHNOLOGY

RESEARCH ARTICLE

Spectroscopic, Vibrational and Topology Analysis of (2R, 3R) - Butanediol bis (Methanesulfonate)

P R Babila[1]*, E S Ashlin[2], G Edwin Sheela[3]

1 Reg.No:19123092132011, Research scholar, Department of Physics and Research Centre, Muslim Arts College (Affiliated to Manonmaniam Sundaranar University, Tirunelveli), Thiruvinthancode, 629 174, Tamilnadu, India
2 Reg.No:19123092132010, Research scholar, Department of Physics and Research Centre, Muslim Arts College, (Affiliated to Manonmaniam Sundaranar University, Tirunelveli), Thiruvinthancode, 629 174, Tamilnadu, India
3 Associate Professor, Department of Physics and Research Centre, Muslim Arts College (Affiliated to Manonmaniam Sundaranar University, Tirunelveli), Thiruvinthancode, 629 174,, Tamilnadu, India

OPEN ACCESS

Received: 15-05-2022
Accepted: 30-09-2022
Published: 07-12-2022

Citation: Babila PR, Ashlin ES, Sheela GE (2022) Spectroscopic, Vibrational and Topology Analysis of (2R, 3R) - Butanediol bis (Methanesulfonate). Indian Journal of Science and Technology 15(45): 2500-2507. https://doi.org/10.17485/IJST/v15i45.1022

* **Corresponding author**.

prbabila@gmail.com

Funding: None

Competing Interests: None

Published By Indian Society for Education and Environment (iSee)

ISSN
Print: 0974-6846
Electronic: 0974-5645

Abstract

Objectives: To find the (2R, 3R)-Butanediol bis (methanesulfonate) (BBM) to be the most bioactive through DFT calculations and multi-spectroscopic investigations. **Methods:** BBM molecule was characterized by multi-spectroscopic investigations (FT-IR, FT-Raman, UV-Vis) and quantum chemical computations employing density functional theory with wB97XD and cam-B3LYP basis functional. **Findings:** The assignments of vibrational spectral features were made with the help of Gar2ped, which incorporates the Scaled Quantum Mechanical Force Field (SQMFF) methodology. The absolute energy gap between the frontier molecular orbitals (HOMO and LUMO) at room temperature and reactivity descriptors confirm that the molecule BBM is chemically active, to realize the charge transfer within the molecule and shows the best bioactive molecule. Moreover, the weak intramolecular interaction and evaluate the intermolecular interaction (hydrogen bonds) were revealed from quantum topological atoms in molecules and reduced density gradient plots. **Novelty:** BBM molecule was found to very good bioactive molecules, given the results of vibrational, topological, quantum computational methods and RDG analysis.

Keywords: BBM; DNA; SQMFF; HOMO; LUMO

1 Introduction

In recent decades, the infectious disorders was caused by bacteria defiant to numerous antimicrobial agents has grown dramatically. A number of factors have been renowned as attributing to this increase, most remarkably misappropriate of antibacterial drugs, which has culminated in higher morbidity and mortality[(1)]. (2R, 3R)- Butanediol bis (methanesulfonate) (BBM) is an alkylsulfonate cross-linking agent and is commonly used as a drug for treating Chronic Myeloid Leukaemia (CML).

It shows a selective immune suppressive effect on bone marrow. BBM is involved in interstrand DNA crosslinking and chromosomal aberration to induce apoptosis through DNA alkylation[2]. Alkylsulfonates were approved by the US Food and Drug Administration for the treatment of chronic myeloid leukaemia[3]. Through Fukwi analysis[4], Benigno et al. have analyzed the chemical reactivity of busulfan and other alkylating DNA cross-linking agents. Nowadays, rational drug design including alkylsulfonates has increased the utilization of spectroscopic and theoretical topological tools for exploring non-covalent interactions (NCIs)[5]. Hence, in the present work, we have reported the spectroscopic characterization and topological, global reactive descriptors of NCIs of BBM molecules. The optimized geometrical parameters, Fukui function analysis, and vibrational assignments for the BBM molecule were analyzed. The HOMO and LUMO energy gaps were used to obtain the reactivity descriptors such as ionization energy (I), electron affinity (A), electronegativity (χ), electrophilicity index (ω), chemical hardness (η), chemical softness (τ) and chemical potential (μ) and are explained. Furthermore, quantum topological atoms in a molecule (QTAIM) analysis were performed to explore the interactions between the non-bonded atoms within 3 Å.

2 Experimental Details

The (2R, 3R)-Butanediol bis(methanesulfonate) (BBM) molecule was purchased from Sigma Aldrich in Bangalore and used without further purification for spectral measurements. The BBM molecule was crystalline in nature. The molecular weight of the BBM molecule was 246.3 kg/m^3. The KBr pellet of a solid sample was 200:1 by applying 4 tones in a hydraulic press. The FT-IR, FT-Raman, and UV-Vis characterization results have been recorded at IIT Saif in Chennai. The Fourier transform infrared (FT-IR) spectrum of BBM was recorded in the MIR region (450–4000 cm^{-1}) on a Perkin Elmer spectrum one LX20000B-SPECTRUM. The spectral data were collected after a cycle of 32 scans at a spectral resolution of 1.0 cm^{-1} using the FT-IR Nernst Glower source. The corrections and primary tasks for signal enhancement and signal averaging were calculated using the multi-tasking OPUS software. FT-Raman spectrum of BBM molecule as recorded in the region 50–4000 cm^{-1} on BRUKER RFS 27: standalone spectrophotometer with Raman module accessory. As an excitation source, an Nd: YAG laser source with a wavelength of 1064 nm was used. The UV-Vis spectrum of BBM in the acetone solvent environment was recorded in the range of 175–3300 nm on a Perkin Elmer LAMBDA 950 UV-Visible Spectrophotometer with a resolution of greater than 0.05 nm and used the Deuterium lamp source at room temperature with the concentration of the sample/solvent of 50 mg: 5 ml.

3 Computational Details

3.1 Quantum chemical computations

Since the crystalline geometry of BBM is not resolved yet, the electronic structure of BBM is retrieved from the pubchem[6] and optimized at the cam-B3LYP/6-311++G (d, p) and wB97XD/6-311++G (d, p) level of approximations using the Gaussian 09W program packages[7] wB97XD and cam-B3LYP functional are range-separate functional with a separation parameter ω is employed. Hence, they accurately predict the minimum energy structure and electronic transitions of hyper-conjugated systems[8]. The local minimum energy of the ground state structure was confirmed from the positive harmonic frequencies predicted at cam-B3LYP/6-311++G (d, p) and wB97XD/6-311++G (d, p) levels. The detailed vibrational assignments of normal modes were obtained using the Gar2Ped program[9]. The isodensity surfaces such as orbital lobes on the HOMO, LUMO were generated with the help of Gaussview 5.0[10]. The TD-DFT calculation was performed for the BBM molecule to find the absorption wavelength corresponding to the electronic transition at wB97XD/6-311++G (d, p) levels and used the PCM solvent model with six electronic states in acetone solvent.

3.2 Topological molecular graph

The pictorial evidence for the intramolecular interactions is obtained from the Quantum Topological Atoms In Molecules (QTAIM) analysis using the AIM All packages[11]. The visualization of molecular graphs was done by AIM 2000. To recognize the strength of the bond, the RDG scatter plot and iso-density surface map were rendered using Multiwfn software[12] along with the VMD GUI programme[13].

4 Results and Discussion

4.1 Optimized geometry and Topological analysis

The optimized molecular structure (Figure 1) and geometrical parameters of the BBM molecule were obtained using DFT calculations at wB97XD/6-311++G (d, p) and B3LYP/6-311++G (d, p) level of approximation. The optimized parameters such as bond lengths, bond angles, and dihedral angles of the BBM molecule are presented in Table 1. Due to the low scattering effect of hydrogen, bond parameters involving hydrogen atoms obtained from X-ray diffraction were found to be lower than the theoretical bond parameters [14]. The average C-H bond length of CH_3 groups calculated using the cam-B3LYP/6-311++G (d, p) method is 1.0936, while the average C-H bond length of CH_3 groups measured in the experiment is 0.91. These bond lengths were deviated by 0.1836Å due to over estimation of bond lengths containing sulphur atoms [15]. The average C-C bond length is nearly 1.5 Å. The C-C-C bond angles of this molecule were calculated as 114.2°. The O-C-C bond angles of BBM were calculated DFT at both WB97XD/6-31++G (d, p) and cam-B3LYP/6-311++G (d, p), showing that deviation by 2° from one another because of different orientations and intramolecular bonding patterns. This indicates that the central atoms undergo sp^2 hybridization [16]. The bond length of S-C bonds was about 1.775 Å. The geometrical bond angles are comparable with respect to the experimental values, except for O_3–S_1–C_{14}, C_9–C_{10}–C_{11}, C_{10}–C_{11}–H_{17}, and O_6–S_1–C_{14}, where the intramolecular charge transfer takes place. The dihedral angles of O_4-C_9-C_{12}-H_{22}, C_{10}-C_9-C_{12}-H_{21}, H_{15}-C_9-C_{12}-H_{20}, O_3-C_{10}-C_{11}-H_{18},and C_9-C_{10}-C_{11}-H_{19} were predicted as~176°. Besides the covalent bonds, the weak non-covalent interactions within the molecule are identified using QTAIM analysis. Geometrical as well as topological parameters are the important parameters to characterize the strength of the hydrogen bond. The topological analysis of atoms in a molecule provides the presence of strong and weak hydrogen bonds in terms of electron density (ρ), Laplacian of electron density ($\nabla^2\rho$) and bond ellipticity (ε) at bond critical points (BCPs) and ring critical points (RCPs). Also, the intramolecular interaction energy (E_{intra}) was calculated using this formula ($E=1/2(V_{BCP})$). In this work, bond ellipticity values of weak hydrogen bond interactions ($C_{12}\cdots O_7$, $O_8\cdots C_{11}$, $O_7\cdots H_{20}$, $C_{11}\cdots C_{13}$) were obtained within the range of (0.0340 a.u-0.4973a.u). This shows the presence of π-bond between them. While the bond ellipticity value of O_7….$H_{20}$is 0.0340 a.u. This predicts that these two interactions fit in to π-type and that they have stronger bond strengths when compared to other interactions [17]. In the bond ellipticity index, one can acquire information about the characteristics of intramolecular hydrogen bonding interactions. To measure the strength of the interactions, the delocalization index (DI) corresponding to their interactions is calculated. The delocalization index is a measure of the average number of electrons shared between the two atoms. The topological parameters of BCPs corresponding to the non-bonded atoms of the BBM molecule at BCP are given in Table S1 and the topological parameters of Ring Critical Point (RCP) are given in Table S2. Figure 2 shows the molecular graph of the BBM molecule at the wB97XD method with the 6-311++G (d,p) basis set. It is clearly seen that the BCPs (small red balls) between the non-bonded atoms predict the presence of interactions like hydrogen bonds and van der Waal forces. The RCPs (small yellow balls) confirm the ring configurations through NCIs. However, the ring configurations of NCIs have a lack of aromaticity.

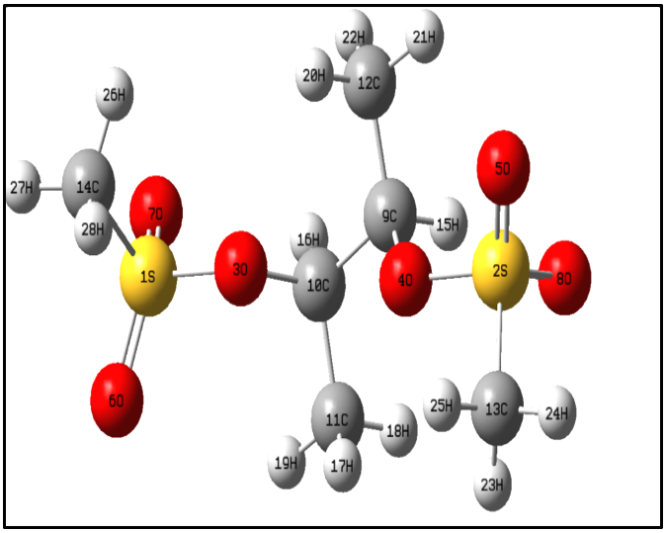

Fig 1.

Table 1. Optimized geometrical parameters of BBM

Bond Length (Å)	DFT		Bond Angles (°)	DFT		Dihedral Angles (°)	DFT	
	wB97XD	cam-B3LYP		wB97XD	cam-B3LYP		wB97XD	cam-B3LYP
S1-O3	1.6191	1.6193	O3-S1-O6	109.0	109.6	O6-S1-O3-C10	91.2	59.3
S1-O6	1.4456	1.4453	O3-S1-O7	108.2	109.2	S1-O3-C10-H16	38.5	11.8
S1-O7	1.4457	1.4461	O3-S1-C14	97.0	97.6	S2-O4-C9-C10	152.8	126.9
S1-C14	1.7749	1.7751	O6-S1-O7	119.0	119.4	S2-O4-C9-C12	-82.4	-108.2
S2-O4	1.6191	1.6193	O6-S1-C14	110.2	109.4	S2-O4-C9-H15	38.5	11.8
S2-O5	1.4456	1.4453	O4-S2-C13	97.0	97.6	O4-C9-C10-O3	67.6	64.9
S2-O8	1.4457	1.4499	O5-S2-O8	119.4	119.0	C12-C9-C10-O3	-54.7	-56.1
S2-C13	1.7749	1.7751	O8-S2-C13	110.3	110.3	C12-C9-C10-C11	-177.1	-177.1
O3-C10	1.4548	1.4554	S1-O3-C10	116.6	118.5	C12-C9-C10-H16	60.1	60.5
O4-C9	1.4548	1.4553	O4-C9-C12	108.5	110.4	H15-C9-C10-O3	-178.6	-178.4
C9-C10	1.5221	1.5185	C10-C9-H15	106.4	106.8	H15-C9-C10-C11	60.1	60.5
C9-C12	1.5132	1.5131	C10-C9-C12	114.2	114.6	H15-C9-C10-H16	-62.8	-61.7
C9-H15	1.095	1.0936	O3-C10-C11	108.5	110.4	O4-C9-C12-H20	-56.6	-57.3
C10-C11	1.5132	1.5144	C9-C10-C11	114.2	114. 6	O4-C9-C12-H21	63.6	63.1
C10-H16	1.0955	1.0935	C10-C11-H17	110.2	110.2	O4-C9-C12-H22	-176.6	-176.5
C11-H17	1.0904	1.0908	C10-C11-H19	109.6	110. 6	C10-C9-C12-H20	63.7	63.2
C11-H18	1.0923	1.0922	H17-C11-H18	108.9	108.0	C10-C9-C12-H21	-176.2	-176.1
C11-H19	1.0905	1.0891	H17-C11-H19	108.6	109.4	C10-C9-C12-H22	-56.3	-55.8
C12-H20	1.0891	1.0890	H18-C11-H19	108.4	109.2	H15-C9-C12-H20	-176.5	-176.5
C12-H21	1.0905	1.0891	C9-C12-H20	110.2	110.2	O3-C10-C11-H17	-56.5	-57.3
C12-H22	1.0923	1.0922	C9-C12-H21	110.6	109. 6	O3-C10-C11-H18	-176.6	-176.5
C13-H23	1.0878	1.0887	C9-C12-H22	109.8	110.2	O3-C10-C11-H19	63.6	63.1
C13-H24	1.0896	1.0902	H20-C12-H22	108.0	108.9	C9-C10-C11-H17	63.7	63.2
C13-H25	1.0878	1.0887	S2-C13-H24	106.1	106.3	C9-C10-C11-H18	-56.3	-55.8
C14-H26	1.0878	1.0868	H23-C13-H25	111.8	111.7	C9-C10-C11-H19	-176.1	-176.2
C14-H27	1.0896	1.0902	S1-C14-H27	106.1	106.3	H16-C10-C11- H18	64.4	64.3
C14-H28	1.0878	1.0887	H26-C14-H28	111.8	111.7	H16-C10-C11-H19	-55.3	-56.0

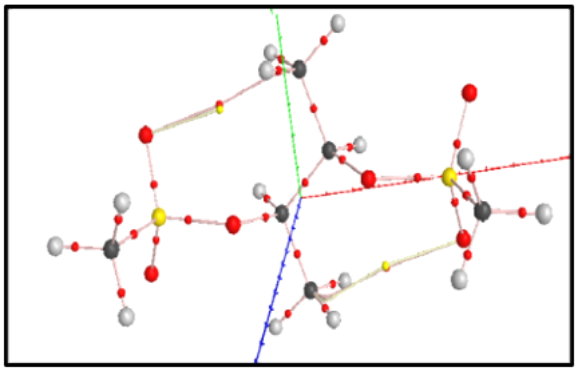

Fig 2.

4.2 Reduced density gradient (RDG) and isodensity surface analysis

The multi-wavefunction analysis in terms of the reduced density gradient graph and iso-density surface was performed to confirm the weak interactions from the AIM molecular graphs of the BBM molecule. Initially, the cube files were generated for the real spatial functions of the product of the second largest Eigen value of the Hessian matrix and electron density ($\lambda^2\rho$) and RDG with the aid of Multiwfn Software. A scatter graph between these two spatial functions with a fixed iso-surface value of about 0.5 a.u is shown in Fig.S5. From the graph, the spike-shaped collection of points in the region from-0.020 a.u to 0.020 a.u and the value of $\lambda^2\rho$ reveals the strength of various interactions in BBM.

In general, the line critical points (3,-1) appear in the chemical bond path between the atoms that have attractive interaction. Fig 3 illustrates the non-bonded interactions in BBM through the isodensity surface. The points enclosed on the right side correspond to hydrogen bonding interactions. The isodensity surface enclosed on the left side represents van der Waals interactions. According to BGR mapping, the isosurface density map shows steric effects in blue and van der Waals interactions in dark green.

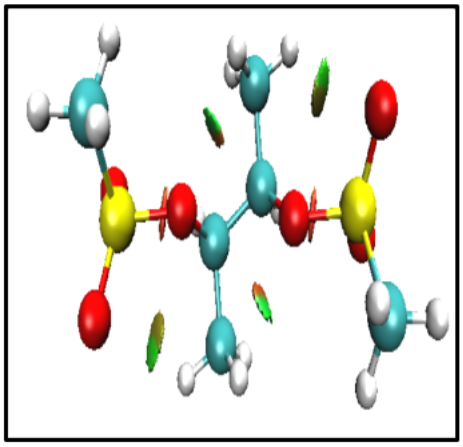

Fig 3.

4.3 Vibrational Assignments

The BBM consists of 28 atoms and has 78 vibrational degrees of freedom. Vibrational spectroscopy techniques are widely used due to their non-destructive analysis of drugs. Figs S6(a) and S6(b) show the experimental FT-IR and FT-Raman spectra, as well as the simulated IR and Raman spectra, at the DFT/cam-B3LYP/6-311++G (d, p) and DFT/wB97XD/6-311++G (d, p) approximation levels of BBM. The vibrational assignments were made by using potential energy distribution (PED) results obtained from Gar2ped software. The theoritical wavenumbers are compared with the experimental wavenumbers along with the vibrational assignments and are depicted in Table: S3.

4.3.1 CH_3 group Vibrations

In general, the asymmetric stretching vibrations of the methyl group occur in the range of 2962-2872cm^{-1} [(18)]. The bands at 3000cm^{-1}, 3020 cm^{-1} in the FT-Raman spectrum and 3022 cm^{-1} in the FT-IR of BBM are attributed to the CH asymmetrical stretching vibrations of S-CH_3. When a methyl group is linked with a sulphur atom, the intensity of these characteristic peaks is not uniform, and a blue shift is observed in wave number. A very strong band found at 2942 cm^{-1} in the Raman spectrum belongs to the asymmetric stretching mode of the methyl group. The repetition of harmonic frequencies (calculated) of CH stretching obtained in the calculation establishes a high degree of degeneracy due to symmetrical entities on both sides of the bond C_9-C_{10}.The C-H in-plane bending wave number frequencies which are useful for the characterization appear in the range of 1000-1300 cm^{-1}was observed at 1080 cm^{-1},1167 cm^{-1} in FT-IR and at 1127 cm^{-1},1162 cm^{-1} in FT-Raman were assigned to bending vibration, which coincides with the scaled values. The asymmetrical and symmetrical deformation modes of the CH_3 group, which is attached to sulphur atoms, produce medium to weak intensity bands in the region 1440-1415 cm^{-1}and 1330-1290 cm^{-1}

4.3.2 SO_3 Vibrations

The asymmetric and symmetric stretching vibrations of the sulfonate group usually appear in the regions of 1430–1330cm^{-1} and 1200–1150cm^{-1}, respectively. In the case of the BBM molecule, the stretching vibrations of the bands at 1167 and 1191 cm^{-1} in the IR spectrum and at 1162cm^{-1} in the Raman spectrum were assigned to asymmetric stretching vibrations. The sulphonate group was identified as weak and medium bands in the region 600-500cm^{-1} in IR and Raman owing to SO_2 deformation.

4.3.3 C-X(S, C) Vibrations

The PED results show that the C-S stretching vibration is highly coupled with the CH_2 rocking vibrations of methane and ethane sulfonates. In the BBM molecule, C-S stretching vibrations were observed at 763 cm^{-1} and 783 cm^{-1}(strong intensity) in the IR spectrum and 764 cm^{-1} (medium intensity) in the Raman spectrum [19]. In the methylsulfonates, there were C-S stretching vibrations coupled with CH_2 vibrations in the range of 800-700cm^{-1} [20].

4.3.4 C-O and C-H Vibrations

The C-O stretching vibrations are usually observed at 1000-700 cm^{-1} [21]. In this study, a strong IR peak at 932 cm^{-1} was assigned to C-O stretching vibrations. In general, the C-H stretching vibration wave numbers are observed in the region at 3077–3003cm^{-1}. The observed and calculated wave number values of C-O and C-H vibrations show good agreement with the literature [22].

4.4 Quantum Reactivity Descriptors

The HOMO-LUMO alkylsulfonate derivatives are used to determine electron transfer and movement. At the wB97XD/6-311++G (d, p) level of approximation, the HOMO and LUMO energies of the BBM molecule were predicted to be 10.4136 eV and 7.9945 eV, respectively. The energy gap between HOMO and LUMO orbitals was predicted to be 2.4191 eV. This reflects that the BBM molecules have given their chemical reactivity and conductivity. The band gap value indicates best for bio active molecules [23]. Fig. S7 shows the HOMO-LUMO of the BBM molecule. The global reactivity descriptors were calculated from the HOMO and LUMO energies and are given in Table 2.

The chemical potential (μ) of the BBM molecule range is -9.8196 eV. Hardness is a direct measure of the stability of the molecule, and softness is a measure of its reactivity. The computed chemical hardness for the BBM molecule range is 1.2096eV. The HOMO and LUMO energy values are used to explain various types of reactions and to predict the most reactive position in combined systems and are descriptors of chemical reactivity associated with the molecular system. The HOMO is located throughout the entire molecule and the LUMO is located approximately SO_3 atoms away. Fig. S8 shows the recorded UV-vis spectrum of BBM in acetone solvent. According to the Planck's radiation relationship between the energy levels involved in the electronic transition and the frequency radiation (E=hc/λ_{max}), the prominent absorption at 250 nm is due to an electron transition from the HOMO to LUMO orbital level, and the experimental wavelength of the BBM molecule concentration has been determined at 255 nm in UV analysis with an oscillator strength of 0.0014 . The λ_{max}wavelength corresponds to π-$\pi^{\star}$ transition. Table S4 shows the wavelength and oscillator strength of the BBM molecule using acetone solvent. The global reactivity descriptor parameter gives the clear information about biological activity of a BBM molecule. The scope of a compound in medical and industrial fields can be ascertained using the chemical softness value, which is predictable to be 0.4133 eV, which indicates the non-toxic nature of the molecule.

Table 2. Global Reactivity Descriptors using HOMO -LUMO orbitals

Global Reactivity Descriptors	DFT/wB97XD / 6- 311++G (d,p)	DFT/ cam-B3LYP / 6-311++G (d,p)
	HOMO-LUMO	HOMO-LUMO
Band gap (eV)	2.4191	3.2462
Ionization energy (I) (eV)	10.4136	10.1603
Electron affinity(A) (eV)	7.9945	6.9192
Chemical Hardness (η) (eV)	1.2096	1.6231
Electro negativity (χ) (eV)	9.2041	8.5397
Chemical Potential (μ) (eV)	-9.2041	-8.5397
Chemical Softness (τ) (eV)-1	0.4133	0.3080
Electrophilicity index (ω) eV	35.0179	22.4651

Table 3. Fukui functions using wB97XD basis set

Atom	Natural atomic charges(q)			Fukui functions				
	N (0,1)	N+1 (-1,2)	N-1 (1,2)	fr+	fr-	fr0	fr+/fr-	fr-/fr+
S1	0.4960	0.0527	-0.0089	0.4433	-0.5049	-0.0308	0.9482	-0.9482
S2	0.4960	0.0520	-0.0089	0.4414	-0.5049	-0.0305	0.9489	-0.9489
O3	-0.1541	0.0062	0.1803	-0.1603	0.3344	0.0871	-0.4947	0.4947
O4	-0.1541	0.0062	0.1802	-0.1603	0.3343	0.087	-0.4946	0.4946
O5	-0.3226	0.0034	0.1152	-0.326	0.4378	0.0559	-0.7638	0.7638
O6	-0.3227	0.0034	0.1153	-0.3261	0.4380	0.0560	-0.7641	0.7641
O7	-0.3212	0.0034	0.1032	-0.3246	0.4244	0.0499	-0.749	0.749
O8	-0.3213	0.0033	0.1031	-0.3246	0.4244	0.0499	-0.749	0.749
C9	0.1214	0.0032	0.0646	0.1182	-0.0568	0.0307	0.175	-0.175
C10	0.1215	0.0033	0.0646	0.1182	-0.0569	0.0307	0.1751	-0.1751
C11	0.0317	0.0520	0.0502	-0.0203	0.0185	-0.0009	-0.0388	0.0388
C12	0.0317	0.0513	0.0502	-0.0196	0.0185	-0.0006	-0.0381	0.0381
C13	0.1487	0.3700	-0.0046	-0.2213	-0.1533	-0.1873	-0.068	0.068
C14	0.1488	0.3768	-0.0046	-0.228	-0.1534	-0.1907	-0.0746	0.0746

4.5 Fukui functions

Hirshfeld charges on the neutral molecule (N) and its anionic (N+1) and cationic (N-1) species produce Fukui functions. Fukui functions derived from Hirshfeld charges provide more accurate sites which are prone to electrophilic or nucleophilic attack. The Fukui functions for the neutral radical, nucleophilic and electrophilic attacks of the BBM molecule can be expressed as f^0,f^+,f^-as described in the reference[24]. The calculated Fukui functions along with relative eletrophilicity and nucleophilicity indices of the BBM molecule are tabulated in Table 9. The S_1 atom of the BBM molecule of two basis sets has a higher f+ value (0.4433) than the other atoms. S_1 indicates that the atomic sites are prone to nucleophilic attack and the f-value of oxygen atoms O_5, O_6, O_7, and O_8 (0.4378, 0.4380, 0.4244, 0.4244) have been reported to be higher than the remaining atoms. This suggests that these are more favourable sites for electrophilic attack and very good for bioactive compound.

5 Conclusion

In this work, a detailed analysis on the structure, vibrational characteristics, and electronic transition, chemical reactivity of BBM were carried out with the aid of spectroscopic techniques and quantum chemical calculations. The optimized geometry calculations of BBM molecule based on DFT with cam-B3LYP and wB97XD basis set. It shows the influence of short range interactions and hyperconjucative effect is mainly reliable for bioactivity of the molecule. The modes of vibrational assignments of the BBM molecule have been done carefully. The frontier molecular orbitals energy gap shows the influence on the intra-molecular charge transfer and bio activity of the given molecule. The prominent stabilization energy of approximately 43 kcal/mol were obtained for the interactions $n_3(O_5) \rightarrow \sigma^*(S_2\text{-}O_4)$, $n_3(O_7) \rightarrow \sigma^*(S_1\text{-}O_3)$ and $n_3(O_8) \rightarrow \sigma^*(S_2\text{-}O_4)$. AIM analysis gives the topological parameters of hydrogen bonds of Bond Critical Point and Ring Critical Point formation. It approaches weak attractive interactions, strong attraction and steric repulsion of the BBM molecule and gives bioactive nature. The UV-vis spectrum of BBM molecule predicts the absorption peak at 255 nm, it belongs to electronic transition from HOMO to LUMO and signifies that the molecule for both stable and bioactive in nature.

6 Acknowledgement

The Authors thank Dr. I. Hubert Joe, Associate Professor of Department of Physics and Kerala University for granting us permission to do computational works in their Research Laboratories.

References

1) Tarika JDD, Shiny CL, Dexlin XDD, Jayanthi DD, Antony S, Beaula TJ. Probing into the outcome of Charge Transfer Interactions and Hyper conjugative Effect on the Antibacterial Molecule 4-dimethylaminopyridine using Spectroscopic Elucidations and DFT Calculations. *Journal of Molecular Structure*. 2022;1251:132059. Available from: https://doi.org/10.1016/j.molstruc.2021.132059.
2) Benigno C, Valdez D, Murray B, Yuan Y, Nieto U, & Borje SP, et al. ABT199/venetoclax potentiates the cytotoxicity of alkylating agents and fludarabine in acute myeloid leukemia cells. *Oncotarget*. 2022;13:319–330. Available from: https://doi.org/10.18632/oncotarget.28193.

3) Karthick T, Tandon P. Computational approaches to find the active binding sites of biological targets against busulfan. *Journal of Molecular Modeling volume*. 2016;22(142). Available from: https://doi.org/10.1007/s00894-016-3015-z.
4) Valdez CB, Yuan B, Murray D, Nieto Y, Popat U, Borje S. Enhanced cytotoxicity of bisantrene when combined with venetoclax panobinostat decitabine and olaparib in acute myeloid leukemia cells. *Leukemia and Lymphoma*. 2022;63:1634–1644. Available from: https://doi.org/10.1080/10428194.2022.2042689.
5) Karthick T, Tandon P, Singh S, Agarwal P, Srivastava A. Characterization and intramolecular bonding patterns of busulfan: Experimental and quantum chemical approach. *Spectrochimica Acta Part A: Molecular and Biomolecular Spectroscopy*. 2017;173:390–399. Available from: https://doi.org/10.1016/j.saa.2016.09.031.
6) National Center for Biotechnology Information (2021). PubChem Compound Summary for CID 71310405, (2R, 3R)-Butanediolbis (methanesulfonate). 2021. Available from: https://pubchem.ncbi.nlm.nih.gov/compound/2R_3R_-Butanediol-bis_methanesulfonate.
7) Frisch MJ, Trucks GW, Schkegel HB, Scuseria GC, Robb MA, Cheeseman JR, et al. Gaussian. Wallingford CT. Gaussian Inc. 2009.
8) Johnson ER, Becke AD. Communication: DFT treatment of strong correlation in 3d transition-meta diatomics. *J Chem Phys*. 2017;146:211105. Available from: https://doi.org/10.1063/1.4985084.
9) Martin JM, Van Alsenoy C. GAR2PED: A Program to Obtain a Potential Energy Distribution from a Gaussian Archive Record. 2007.
10) Dennington TKR, Millam J. GaussView Version 5. Shawnee Mission. KS. Semichem Inc. 2009.
11) Biegler-Konig F, Schonbohm J, Bayles D. AIM2000-a program to analyze and visualize atoms in molecules. *J ComputChem*. 2001;22(5):545–549. Available from: https://www.scirp.org/(S(lz5mqp453edsnp55rrgjct55))/reference/ReferencesPapers.aspx?ReferenceID=980528.
12) Lu T, Chen FF. Multiwfn: A multifunctional wavefunction analyzer. *Journal of Computational Chemistry*. 2012;33(5):580–592. Available from: https://doi.org/10.1002/Jcc.22885.
13) Humphrey W, Dalke A, Schulten K. VMD: Visual molecular dynamics. *Journal of Molecular Graphics*. 1996;14(1):33–38. Available from: https://doi.org/10.1016/0263-7855(96)00018-5.
14) Srivastava R, Al-Omary FAM, El-Emam AA, Pathak SK, Karabacak M, Narayan V, et al. A combined experimental and theoretical DFT (B3LYP, CAM-B3LYP and M06-2X) study on electronic structure, hydrogen bonding, solvent effects and spectral features of methyl 1H-indol-5-carboxylate. *Journal of Molecular Structure*. 2017;1137:725–741. Available from: https://doi.org/10.1016/j.molstruc.2017.02.084.
15) Kaya Y, Kucuk I, Kaya AA. Conformational, spectroscopic, optical, physicochemical and molecular docking study of 4-methoxy-benzaldehyde oxime and 4-hydroxy-3-methoxy-benzaldehyde oxime. *Physics and Chemistry of Liquids*. 2020;58(1):77–93. Available from: https://doi.org/10.1080/00319104.2018.1550775.
16) Silvi MB, Alikhani C, & Remi Chauvin L. Topological Approaches of the Bonding in Conceptual Chemistry. *Applications of Topological Methods in Molecular Chemistry*. 2016;22:1–20. Available from: https://doi.org/10.1007/978-3-319-29022-5_1.
17) Firme LC, Araujo MD. Revisiting electronic nature and geometric parameters of cyclophanes and their relation with stability-DFT QTAIM and NCI study. *Computational and Theoretical Chemistry*. 2018;1135:18–27. Available from: https://doi.org/10.1016/j.comptc.2018.05.008.
18) Tarika JDD, Dexlin XDD, Kumar A, Rathika A, Jayanthi DD, Beaula TJ. Computational Insights On Charge and Non-covalent Interactions of Antibacterial Compound 4-dimethylaminopyridinium pyridine-2-carboxylate pentahydrate. *Journal of Molecular Structure*. 2022;1256:132525. Available from: https://doi.org/10.1016/j.molstruc.2022.132525.
19) Kosar B, Albayrak C. Spectroscopic investigations and quantum chemical computational study of (E)-4-methoxy-2-[(p-tolylimino)methyl]phenol. *Spectrochimica Acta Part A: Molecular and Biomolecular Spectroscopy*. 2011;78(1):160–167. Available from: https://doi.org/10.1016/j.saa.2010.09.016.
20) Chakraborty D, & Pratim Kumar Chattaraj. Conceptual density functional theory based electronic structure principles. *Chemical Sciences*. 2021;12:6264–6279. Available from: https://doi.org/10.1039/DOSCO7017C.
21) Kumar V, Jain G, Kishor S, Ramaniah LM. Chemical reactivity analysis of some alkylating drug molecules – A density functional theory approach. *Computational and Theoretical Chemistry*. 2011;968(1-3):18–25. Available from: https://doi.org/10.1016/j.comptc.2011.04.034.
22) Choudhary N, Bee S, Gupta A, Tandon P. Comparative vibrational spectroscopic studies, HOMO–LUMO and NBO analysis of N-(phenyl)-2,2-dichloroacetamide, N-(2-chloro phenyl)-2,2-dichloroacetamide and N-(4-chloro phenyl)-2,2-dichloroacetamide based on density functional theory. *Computational and Theoretical Chemistry*. 2013;1016:8–21. Available from: https://doi.org/10.1016/j.comptc.2013.04.008.
23) Cedillo A, Chattaraj KP, Parr GR. Atoms-in-molecules partitioning of a molecular density. *Internationl Journal of Quantum Chemistry*. 2000;77(1):403–407. Available from: https://doi.org/10.1002/(SICI)1097-461X(2000)77:1%3C403::AID-QUA40%3E3.0.CO;2-9.
24) Manjushaa P, Prasana JC, & Fathima Muthu S, Rizwana B. Spectroscopic elucidation (FT-IR, FT-Raman and UV-visible) with NBO, NLO, ELF, LOL, drug likeness and molecular docking analysis on 1-(2-ethylsulfonylethyl)-2-methyl-5-nitro-imidazole: An antiprotozoal agent. *Comput BioChemistry*. 2020;88:107330. Available from: https://doi.org/10.1016/j.compbiolchem.2020.107330.